# Energy level alignment of $Cu(In, Ga)(S, Se)_2$ absorber compounds with $In_2S_3$, $NaIn_5S_8$, and $CuIn_5S_8$ Cd-free buffer materials

Elaheh Ghorbani,[1,*] Paul Erhart,[2] and Karsten Albe[1]

[1] *Fachgebiet Materialmodellierung, Institut für Materialwissenschaft, TU Darmstadt, Otto-Berndt-Straße 3, D-64287 Darmstadt, Germany*

[2] *Department of Physics, Chalmers University of Technology, SE-412 96 Gothenburg, Sweden*

(Received 12 April 2019; revised manuscript received 21 June 2019; published 15 July 2019)

Motivated by environmental reasons, $In_2S_3$ is a promising candidate for a Cd-free buffer layer in $Cu(In, Ga)(S, Se)_2$ (CIGSSe)-based thin-film solar cells. For an impactful optimization of the $In_2S_3$ alternative buffer layer, however, a comprehensive knowledge of its electronic properties across the absorber-buffer interface is of foremost importance. In this respect, finding a favorable band offset between the absorber and the buffer layers can effectively reduce the carrier recombination at the interface and improve open-circuit voltage and fill factor, leading to higher conversion efficiencies. In this study, we investigate the band alignment between the most common CIGSSe-based absorber compounds and $In_2S_3$. Furthermore, we consider two chemically modified indium sulfide layers, $NaIn_5S_8$ and $CuIn_5S_8$, and we discuss how the formation of these secondary phases influences band discontinuity across the interface. Our analysis is based on density functional theory calculations using hybrid functionals. The results suggest that Ga-based absorbers form a destructive clifflike conduction-band offset (CBO) with both pure and chemically modified buffer systems. For In-based absorbers, however, if the absorber layer is Cu-poor at the surface, a modest favorable spikelike CBO arises with $NaIn_5S_8$ and $CuIn_5S_8$.

DOI: 10.1103/PhysRevMaterials.3.075401

## I. INTRODUCTION

$Cu(In, Ga)(S, Se)_2$ (CIGSSe) is widely used as a light absorber in efficient and inexpensive thin-film solar cells. Recently, the world record efficiency of CIGSSe cells reached 22.9% [1], which was attained mainly through optimizing the light absorber layer via alkali-treatment [1–7]. To further boost device performance, the *n*-type buffer layer and the band alignment across the absorber-buffer interface have to be optimized and resolved. To date, CdS is the most widely used buffer-layer material in CIGSSe-based thin-film solar cells. Environmental concerns due to the toxicity of Cd led, however, to the development of several Cd-free buffer layers [8–10]. In this context, $\beta$-$In_2S_3$ emerged as one of the most relevant substituents for CdS. However, little is known about $In_2S_3$, and many of its properties, including band offsets to CIGSSe absorbers, are not well understood yet.

The band offset at the *pn*-junction (and in general at all heterojunctions) refers to the discontinuity between the valence- and conduction-band edges of the two semiconductors. The band-edge offsets have a pronounced impact on solar cell performance, mainly through facilitating or eliminating interface recombination. The conduction bands of the absorber and buffer materials can either be aligned, i.e., no offset exists, or discontinuous. In the latter case, the offsets of the conduction bands either form a spike (where the conduction band of the buffer layer is above that of the absorber layer) or they have a clifflike (where the conduction band of the buffer layer is below that of the absorber layer) discontinuity at the junction. While a moderate spikelike offset (0.0–0.3 eV) can play a positive role and suppress recombination, the clifflike offset triggers charge recombination at the interface and reduces the interface band gap. For more details on the energy band diagram in spike and cliff conformations, we refer the reader to Ref. [11].

Previous studies [12–14] indicate that the conduction-band offset (CBO) for high efficiency CdS/CIGSe-based thin-film solar cells is mainly flat, with a small spike. We note that in order to get close to the efficiencies obtained with CdS-buffered cells, reaching a favorable CBO in $In_2S_3$-buffered devices is crucial. As reported by Schulmeyer *et al.* [15], the conduction-band minimum (CBM) of $In_2S_3$ at the interface between $In_2S_3$ and Cu-poor $CuGaS_2$ is placed 0.56 eV below that of $CuGaS_2$, forming an undesirable clifflike band diagram. According to the literature [16–19], the CIGSSe-$In_2S_3$ interface is, however, heavily intermixed, containing a large concentration of Cu and Na ions that migrate from the absorber into the $In_2S_3$ buffer layer. After entering $In_2S_3$, Na and Cu cause the formation of secondary phases at the buffer side of the interface [20,21].

In 2016, Bär *et al.* [22] observed the existence of a $CuIn_5S_8$-like built-in buffer that modified the interface structure chemically and led to a small desirable spikelike CBO. Recently, Hauschild *et al.* [20] used ultraviolet photoelectron spectroscopy (UPS) and inverse photoemission spectroscopy to determine the conduction-band offset between $CuIn(S,Se)_2$ and Na-doped $In_2S_3$ ($In_xS_y$:Na). Their results confirm a spikelike CBO, suggesting $In_xS_y$:Na to be a promising Cd-free buffer layer.

The objective of this work is to improve the current knowledge of valence- and conduction-band lineup between

*ghorbani@mm.tu-darmstadt.de



©2019 American Physical Society

TABLE I. Comparison between experimentally measured and calculated equilibrium lattice constants, $a$ and $c$, and band gaps, $E_g$, for the systems under study. Experimentally reported values are shown in parentheses and are taken from Refs. [23–29].

| | $a$ (Å) | $c$ (Å) | $E_g$ (eV) |
|---|---|---|---|
| $CuInSe_2$ | 5.84 (5.78) | 11.73 (11.82) | 1.10 (1.04) |
| $CuGaSe_2$ | 5.64 (5.61) | 11.10 (11.02) | 1.68 (1.68) |
| $CuInS_2$ | 5.56 (5.52) | 11.21 (11.13) | 1.53 (1.52) |
| $CuGaS_2$ | 5.36 (5.35) | 10.55 (10.46) | 2.44 (2.43) |
| $CuIn_5Se_8$ | 11.67 (11.44) | 11.68 (11.62) | 1.32 (1.23) |
| $CuGa_5Se_8$ | 11.07 (11.43) | 10.95 (10.94) | 1.62 (1.82) |
| $CuIn_5S_8$ | 10.77 (10.68) | 10.76 (10.68) | 1.66 (1.50) |
| $NaIn_5S_8$ | 10.95 (10.85) | 11.02 (10.85) | 2.56 (2.40) |
| $In_2S_3$ | 7.68 (7.62) | 32.91 (32.36) | 2.03 (2.03) |

CIGSSe-based absorbers and $In_2S_3$-based buffer materials. To this end, we studied the valence-band offset (VBO) and CBO between six different CIGS-based absorber compounds and $In_2S_3$. In addition, motivated by the occurrence of Na and Cu in the crystalline matrix of $In_2S_3$, we performed calculations for chemically modified buffer layers, namely $NaIn_5S_8$ and $CuIn_5S_8$, as well. The effects of including Ga, S, and excess Cu in the surface of absorber layer are analyzed based on electronic density of states of the studied materials.

## II. CALCULATION METHODS

All calculations were performed within the framework of density functional theory DFT using the range-separated Heyd-Scuseria-Ernzerhof hybrid functional with a mixing parameter of $\alpha = 0.25$ and an exchange-screening length of $\omega = 0.13$ Å$^{-1}$ [30] as implemented in the Vienna Ab-initio Simulation Package [31,32]. This hybrid functional setup has already delivered an accurate description of the band gap for different CIGSSe-based compounds as well as $In_2S_3$ [33–36]. A plane-wave cutoff energy 400 eV was applied for all calculations. $\Gamma$-centered $k$-point grids of $4 \times 4 \times 1$, $4 \times 4 \times 2$, $2 \times 2 \times 2$, and $2 \times 2 \times 2$ were used for sampling Brillouin zones of defect spinel-like $In_2S_3$, tetragonal Cu(In,Ga)(S,Se)$_2$, cubic Cu(In,Ga)$_5$Se$_8$ ordered vacancy compounds, and cubic (Na,Cu)$In_5S_8$, respectively. The calculated bulk properties of different chalcopyrite compounds, $In_2S_3$, $CuIn_5S_8$, and $NaIn_5S_8$, are listed in Table I and their crystal structures are shown in Fig. 1. The good description of the band gaps of these bulk systems suggests that the hybrid DFT approach employed here is also reliable for studying their band offsets.

To determine band offsets accurately, the band edges of absorber and buffer systems must be properly aligned with respect to a common reference level. To this end, the band positions were aligned with respect to the core-level energies according to

$$\Delta E_v(X-Y) = \Delta E_{v,c'}(Y) - \Delta E_{v,c}(X) + \Delta E_{c,c'}(X-Y), \quad (1)$$

where $\Delta E_{v,c'}(Y)$ and $\Delta E_{v,c}(X)$ denote the energy difference between the valence-band maximum (VBM) and the core-level energy of the bulk $Y$ and $X$ compounds, respectively. $\Delta E_{c,c'}(X-Y)$ is the energy difference between core levels of the $X$ and $Y$ compounds at the $X-Y$ interface. The CBOs were then calculated using the relation

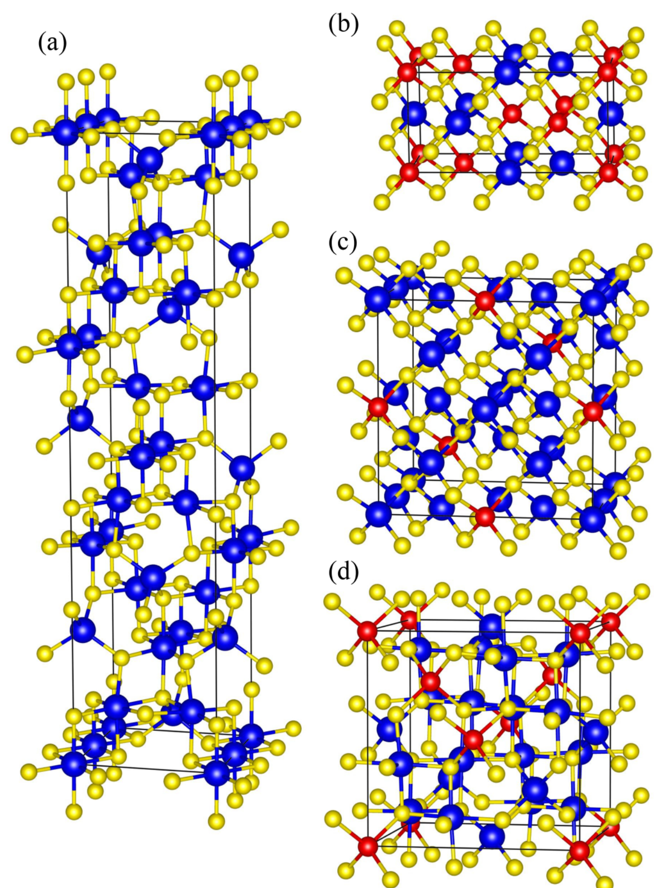


FIG. 1. Unit cells of (a) defect spinel-like $In_2S_3$, (b) tetragonal Cu(In, Ga)(S, Se)$_2$, (c) cubic Cu(In,Ga)$_5$Se$_8$ ordered vacancy compounds, and (d) cubic (Na,Cu)$In_5S_8$. Red spheres represent Na/Cu, blue spheres represent In/Ga, and yellow spheres represent S/Se atoms.

$$\Delta E_c(X-Y) = \Delta E_g(X-Y) - \Delta E_v(X-Y), \quad (2)$$

where $\Delta E_g(X-Y)$ is the difference in band gap between the two compounds.

The interface between Cu-based absorbers and the buffer is highly lattice-mismatched. As a result, in order to include interfacial strain or dipole effects in band alignment calculations, we must deal either with a moderate size but unreasonably large interface strain, or extremely large interfaces with a moderate contribution of strain. While the former case is unreliable, in the latter, interface configurations contain about 1000 atoms and cannot be modeled within a reasonable amount of computer time. Therefore, in this work we focus on bulk-intrinsic (or natural) band lineups between the Cu-based absorber materials and buffer compounds, i.e., $\Delta E_{c,c'}(X-Y) = 0$. In our calculations, the binding energy of the Cu 2$s$ state was used for alignment between the Cu-containing compounds. The energy band alignments between $NaIn_5S_8$, $CuIn_5S_8$, and $In_2S_3$ and their relative positions to the VBM and CBM of $CuInSe_2$ were calculated with respect to the In 3$s$ core state.

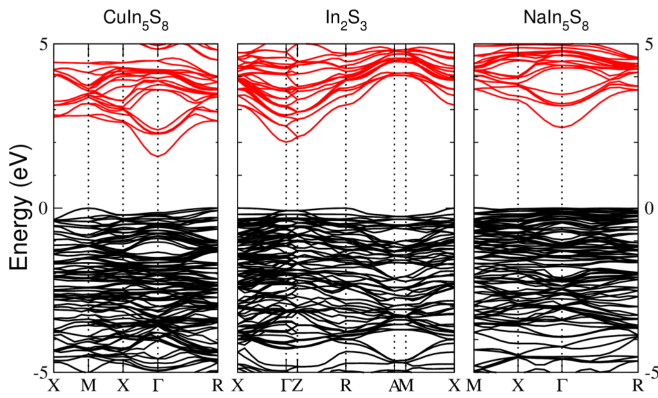


FIG. 2. Electronic band structure of $CuIn_5S_8$ (left), $In_2S_3$ (middle), and $NaIn_5S_8$ (right). Occupied and unoccupied levels are shown as black and red lines, respectively. The zero of energy is set to the bulk VBM of each structure.

## III. RESULTS AND DISCUSSIONS

The electronic band structures of the three buffer materials are shown in Fig. 2. Strictly speaking, both $In_2S_3$ and $CuIn_5S_8$ exhibit an indirect band gap. $In_2S_3$ has a nearly direct band gap, in which the CBM and VBM are located at the Γ and $X$ points, respectively, and the highest valence band at the Γ point is only 0.06 eV lower than at the $X$ point. Therefore, $In_2S_3$ can be considered as a nearly direct band-gap material. As Fig. 2 shows, the uppermost part of the VB in $In_2S_3$, $CuIn_5S_8$, and $NaIn_5S_8$ structures is nearly flat. The bottom of the CB, however, shows considerable dispersion. This feature is most pronounced in $NaIn_5S_8$ and forms the basis for the high electron mobility of these systems. Electrical conductivity measurements of $In_2S_3$, $NaIn_5S_8$, and $CuIn_5S_8$ suggest that inclusion of Na and Cu in $In_2S_3$ leads to higher and lower electrical conductivity of the films, respectively [38].

Figure 3 shows the calculated band alignment of $In_2S_3$, $NaIn_5S_8$, and $CuIn_5S_8$ with the common CIGSSe-based chalcopyrite systems. To gain further insights regarding the origin of the band offsets, we first analyze the electronic density of states of each compound (Fig. 4). The upper valence bands of both Cu-rich and Cu-poor absorbers originate from hybridization between Cu $d$ and S/Se $p$ orbitals. Cu $d$ has two sharp peaks in the VB of the Cu-rich compounds (i.e., $CuInSe_2$, $CuInS_2$, $CuGaSe_2$, and $CuGaS_2$), which are separated by a small gap and correspond to bonding (lower peak) and antibonding (upper peak) states between Cu $d$ and S/Se $p$ states. These peaks are slightly closer to the VBM in In compounds compared to Ga compounds, in agreement with Ref. [39]. In $CuInSe_2$, for instance, Cu $d$ peaks are found at 2.42 and 3.68 eV below the VBM, whereas in $CuGaSe_2$ they are slightly deeper at 2.52 and 3.74 eV below the VBM.

Moving from Cu-rich to Cu-poor structures, some of the anions do not participate in bonding. Hence, these S/Se atoms are effectively undercoordinated [40] and the $p$-$d$ repulsion becomes weaker. The reduced $p$-$d$ repulsion is associated with a pronounced lowering of the VBM in Cu-poor compounds compared to Cu-rich ones, which is in line with the report by Zhang *et al.* [41].

In $In_2S_3$, the upper VB is formed by mixing of In $d$ and S $p$ orbitals. Due to the large participation of In and the absence of Cu cations, the position of the VBM of $In_2S_3$ relative to $CuInSe_2$ is lowered substantially [$\Delta E_{VB}(In_2S_3 - CuInSe_2) = 1.26$ eV]. We have shown in a previous study [21] that due to the existence of a massive driving force for diffusion of Cu and Na ions from the absorber into the $In_2S_3$ buffer layer, Cu- and/or Na-containing secondary phases are bound to form on

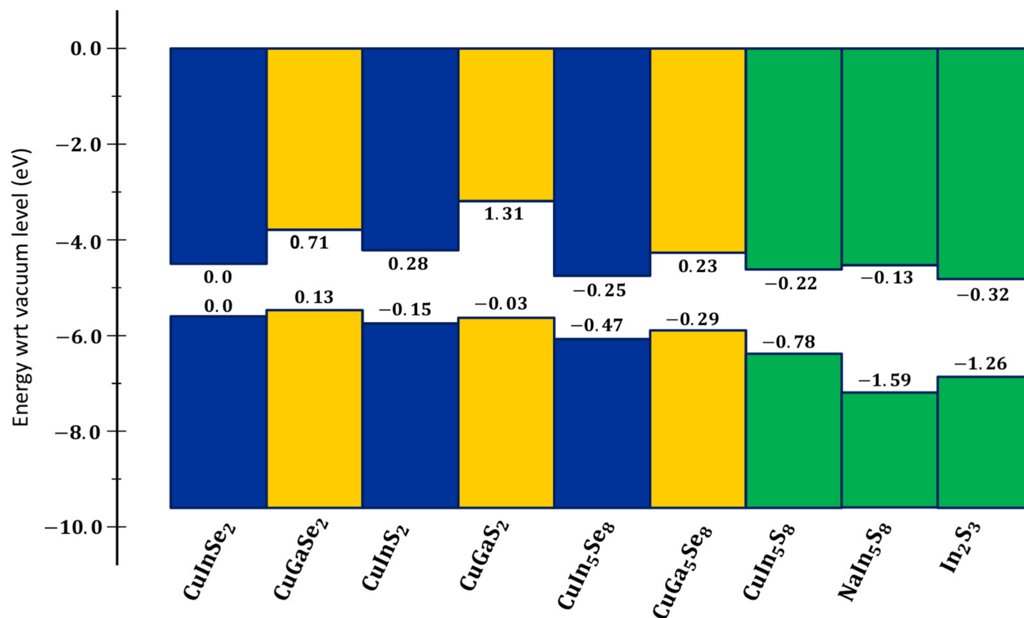


FIG. 3. Calculated band lineups of bulk materials. For each material, the lower and upper numbers indicate, respectively, the position of the VBM and the CBM with respect to $CuInSe_2$ in eV. The VBM of $CuInSe_2$ lies at a value in energy scale that corresponds to the ionization potential of the (110) surface of $CuInSe_2$ (5.58 eV [37]).

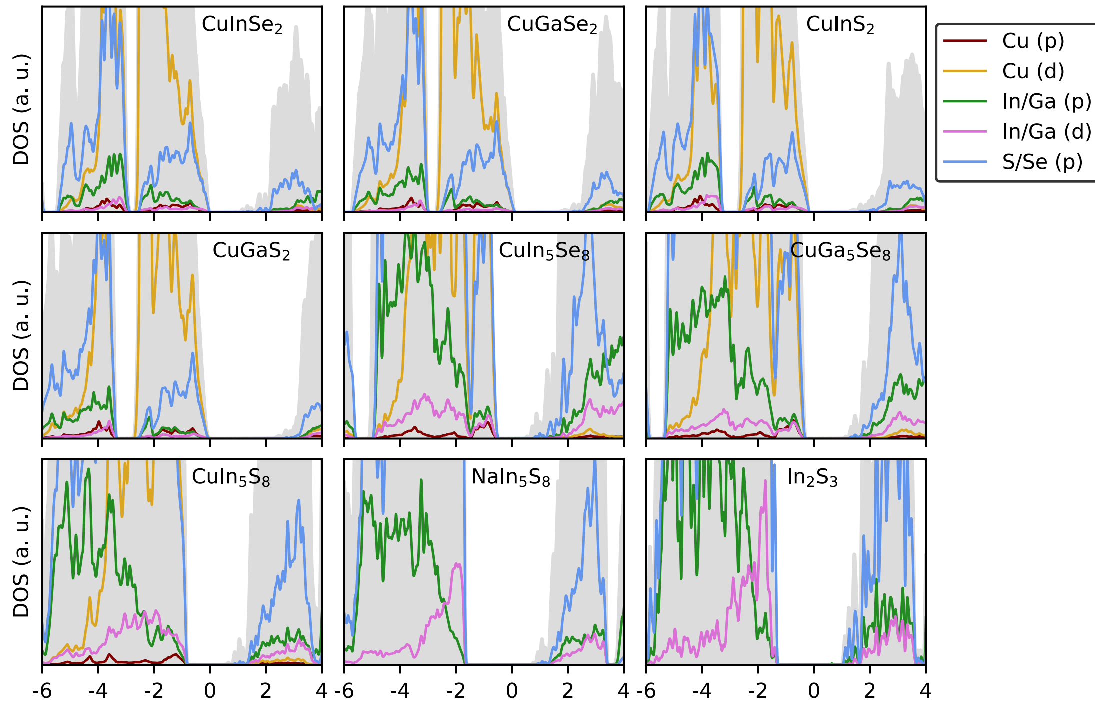


FIG. 4. Electronic total and local density of states (DOS) of absorber (top and middle panels) and buffer (bottom panel) compounds. The energy scales are aligned with respect to the VBM of $CuInSe_2$. The gray shaded area shows the total DOS of each compound.

the buffer side of the absorber-buffer interface. Knowledge of the alignment of energy levels of $CuIn_5S_8$ and $NaIn_5S_8$ with the absorber materials is therefore essential. Upon diffusion of Cu into the crystalline matrix of $In_2S_3$ and the formation of a $CuIn_5S_8$ secondary phase, the Cu $d$–S $p$ repulsion reduces the gap and raises the VBM. On the other hand, Na has empty $d$ orbitals, which are higher than S $p$ orbitals, as a result of which $NaIn_5S_8$ lacks $d$-$p$ repulsion.

As shown in Fig. 3, if one replaces In by Ga, the CB position is shifted to higher energies, while the VB is less affected [42,43]. This feature suggests more negative clifflike offsets between the Ga-containing chalcopyrites and buffer materials compared to In-containing ones. We also see that the CBM is significantly higher for Cu-rich compounds (i.e., $CuGaSe_2$ and $CuGaS_2$) compared to that of Cu-poor compounds ($CuGa_5Se_8$), which results in a significantly larger CBO cliff in Cu-rich ones. This suggests that when buffering the cell with $In_2S_3$, $NaIn_5S_8$, or $CuIn_5S_8$, incorporation of Ga in the absorber side of the interface must be avoided.

A comparison between the compounds with common cations and different anions shows that, as expected, when increasing the atomic number of the anion (from S to Se), the VB moves upward while the CB moves downward, resulting in a decreased band gap. The change in VB position originates from the fact that the energy of the $3p$ orbital of Se is larger than the energy of the $2p$ orbital of S, leading to larger anion-cation bond lengths and a higher VBM energy. The reduction in the CBM, on the other hand, is correlated with the increase in the volume of the Se compounds [44].

The values of CBO between different heterointerfaces are listed in Table II. These numbers have been derived by making use of the transitivity rule,

$$\Delta E_{\mathrm{CB}}(X-Y)=\Delta E_{\mathrm{CB}}^{X-Z}-\Delta E_{\mathrm{CB}}^{Y-Z}, \tag{3}$$

where $Z$ represents $CuInSe_2$, and $X$ and $Y$ represent two different compounds. In 2004, Schulmeyer *et al.* deposited pure $In_2S_3$ on Cu-poor $CuGaSe_2$ and investigated the electronic properties of the absorber-buffer heterointerface by means of the x-ray photoemission spectroscopy (XPS) [15]. From the reported band gap of their Cu-poor absorber (1.68 eV), it can be inferred that their Cu-poor sample had a $CuGa_5Se_8$-like stoichiometry. The XPS VBM of the Cu-poor absorber was determined to lie 0.78 eV above that of $In_2S_3$ and the CBO has been calculated to be −0.56 eV. Our calculated CBO for the $CuGa_5Se_8$-$In_2S_3$ interface is −0.55 eV, in excellent agreement with XPS results. In addition, a very small dipole

TABLE II. Calculated values of CBOs between different absorber materials, as specified in the first column, and $In_2S_3$, $CuIn_5S_8$, and $NaIn_5S_8$ buffer materials. Note that only the $CuIn_5Se_8$ absorber has a positive CBO with the chemically modified $CuIn_5S_8$ and $NaIn_5S_8$ buffer systems.

| | $In_2S_3$ | $CuIn_5S_8$ | $NaIn_5S_8$ |
|---|---|---|---|
| $CuInSe_2$ | −0.32 | −0.22 | −0.13 |
| $CuGaSe_2$ | −1.03 | −0.93 | −0.84 |
| $CuInS_2$ | −0.6 | −0.5 | −0.41 |
| $CuGaS_2$ | −1.63 | −1.53 | −1.44 |
| $CuIn_5Se_8$ | −0.07 | +0.03 | +0.12 |
| $CuGa_5Se_8$ | −0.55 | −0.45 | −0.36 |

potential was found in their work, which gives us confidence that inclusion of the interfacial term in Eq. (1) does not substantially alter our result.

As mentioned above, to achieve the best device performance, the CBO needs to be positive (spikelike) across the absorber-buffer *pn*-junction. As illustrated in Fig. 3 and shown in Table II, the CBOs between all Cu-rich compounds and $In_2S_3$, $NaIn_5S_8$, and $CuIn_5S_8$ buffer materials are negative, thus demonstrating a destructive clifflike potential change at the interface. It is, however, well documented that the absorber layer is Cu-poor close to the interface and the absorber surface is not the stoichiometric $CuInSe_2$ [45–49]. $CuIn_3Se_5$ and $CuIn_5Se_8$ are the two common Cu-deficient ordered vacancy compounds that are suggested to form at the surface of the absorber layer [41,45,50]. Since there is no precise structural information available for $CuIn_3Se_5$, this phase has not been considered in our calculations.

Now, we put our focus on the CBOs between $CuIn_5Se_8$ and the three buffer materials. When the absorber layer is Cu-poor and In-containing, the CBOs across $CuIn_5Se_8$-$CuIn_5S_8$ and $CuIn_5Se_8$-$NaIn_5S_8$ heterostructures are spikelike with small positive values of 0.03 and 0.12 eV, respectively. The CBO between $CuIn_5Se_8$ and $In_2S_3$ is a small cliff of −0.07 eV. Hauschild *et al.* [20] studied the band offsets between an In-containing absorber with a band gap of 1.44 eV and a Na-containing $In_xS_y$ buffer with a band gap of 2.60 eV. According to their reported band gaps, we speculate that their formed interface is very similar to the $CuIn_5Se_8$-$NaIn_5S_8$ interface, with a small contribution of sulfur on the absorber side of the interface. According to their report, the CBO at the absorber-buffer interface has a spike of 0.32 eV, in very good agreement with our calculations. The small discrepancy can be caused by the S content in their absorber and also the existence of small interface dipoles. With regard to the very good agreement between our results and the available XPS and UPS measurements, it is noted that the interface dipole and strain contributions to the energy band alignments are very small, and for these heterostructures the lineup is dominated by bulk effects.

To have a better control over band lineups, in the following we discuss several possible scenarios that can affect band edges. As discussed, the CBO between $CuIn_5Se_8$ and $NaIn_5S_8$ is a favorable spike of +0.12 eV. However, having higher Cu concentration on the absorber side of the interface (for instance, $CuIn_3Se_5$ or $CuInSe_2$ phases) can change the band offset conformation from the desired slight spike to a harmful cliff. To surmount the negative effect of Cu in displacing the CB edge of the absorber to higher energies, we suggest to dope $In_2S_3$ with higher concentrations of Na, which in return shifts the CB of the buffer layer upward, too. In this case, in order to prevent construction of a negative CBO at the absorber-buffer interface, the Na/Na+In ratio in the buffer layer needs to increase from 0.17, corresponding to that of $NaIn_5S_8$. We note that the same analysis applies also for the cases in which a high S and/or Ga content exists at the Cu-poor absorber. This condition can lead to the formation of $Cu(In,Ga)_5Se_8$ or $CuIn_5(S,Se)_8$ mixed phases. Again, to overcome the conduction-band upward shifts caused by the presence of S and Ga, a higher Na content is recommended. Alternatively, substituting In with smaller group-III cations (for instance, Ga) and the formation of an $In_{1-x}Ga_xS_3$ solid solution is another possible way of shifting the CBM of the buffer layer to higher energies [51–54].

Depending on the preparation technique, a considerable amount of oxygen can be present in $In_2S_3$ [8,55]. In Zn- and Cd-based common-cation materials [52,56,57], going from Se to S mainly affects the VB edge through shifting it downward. However, due to the large difference in the bond length and the crystal structure of sulfides compared to oxides, moving from S to O causes a significant downward shift in both the VBM and the CBM. In this respect, we expect that doping $In_2S_3$ with high amounts of O and forming an $In_2O_xS_{1-x}$ alloy will lead to a downward shift of both the valence- and conduction-band edges of the buffer layer. This can stimulate a deep cliff conformation resulting in large carrier recombination at the interface.

## IV. CONCLUSIONS

Using *ab initio* first-principles calculations, we have investigated the band discontinuity across the absorber-buffer interface in CIGSSe-based thin-film solar cells. The absorber systems considered in this work were $CuInSe_2$, $CuInS_2$, $CuGaSe_2$, $CuGaS_2$, $CuIn_5Se_8$, and $CuGa_5Se_8$. $In_2S_3$, $CuIn_5S_8$, and $NaIn_5S_8$ were considered as the Cd-free buffer materials. In summary, the results imply that when buffering CIGSSe with $In_2S_3$, the surface of the absorber layer must be Ga-free with a minimum concentration of S ions. This is because in Ga- and S-containing alloys, the CBM is placed at higher energies, which leads to a negative clifflike CBO across the absorber-buffer interface. Based on the obtained results, at the $CuIn_5Se_8$-$CuIn_5S_8$ interface the CBO is almost flat and it has a small spike of 0.12 eV at the $CuIn_5Se_8$-$NaIn_5S_8$ interface. Since both $CuIn_5S_8$ and $NaIn_5S_8$ achieve a better band alignment with the Cu-poor absorber, their incorporation as a Cd-free buffer can localize electron and holes at different sides of the interface and suppress unwanted recombination, leading to higher device efficiencies. Considering its direct band gap, higher transparency, and improved electrical conductivity, $NaIn_5S_8$ would be a more relevant candidate than $CuIn_5S_8$. We note that our natural band lineups demonstrate very good agreement with existing experimental data, which suggests that the effects of the interface dipole and strain are screened and do not play a major role in band alignment.

## ACKNOWLEDGMENTS

This work has been financially supported by German Federal Ministry for Economic Affairs and Energy (BMWi) through EFFCIS project under Contract No. 0324076D. E.G. would like to thank the Hessian Competence Center for High Performance Computing—funded by the Hesse State Ministry of Higher Education, Research and the Arts—for helpful advice. P.E. gratefully acknowledges support in the form of a Fellowship by the Knut and Alice Wallenberg Foundation. Fruitful discussions with Clemens Heske are gratefully acknowledged. The computing time was provided by Jülich Supercomputing Center (Project HDA30) and Lichtenberg HPC computer resources at TU Darmstadt.

[1] R. Kamada, T. Yagioka, S. Adachi, A. Handa, K. F. Tai, T. Kato, and H. Sugimoto, New world record $Cu(In, Ga)(Se, S)_2$ thin film solar cell efficiency beyond 22%, *2016 IEEE 43rd Photovoltaic Specialists Conference (PVSC)* (IEEE, Piscataway, NJ, 2016), p. 1287.

[2] D. Rudmann, A. F. da Cunha, M. Kaelin, F. Kurdesau, H. Zogg, A. N. Tiwari, and G. Bilger, Efficiency enhancement of $Cu(In,Ga)Se_2$ solar cells due to post-deposition Na incorporation, Appl. Phys. Lett. **84**, 1129 (2004).

[3] A. Laemmle, R. Wuerz, and M. Powalla, Efficiency enhancement of $Cu(In,Ga)Se_2$ thin-film solar cells by a post-deposition treatment with potassium fluoride, Phys. Status Solidi RRL **7**, 631 (2013).

[4] A. Chirila, P. Reinhard, F. Pianezzi, P. Bloesch, A. R. Uhl, C. Fella, L. Kranz, D. Keller, C. Gretener, H. Hagendorfer, D. Jaeger, R. Erni, S. Nishiwaki, S. Buecheler, and A. N. Tiwari, Potassium-induced surface modification of $Cu(In,Ga)Se_2$ thin films for high-efficiency solar cells, Nat. Mater. **12**, 1107 (2013).

[5] P. Jackson, R. Wuerz, D. Hariskos, E. Lotter, W. Witte, and M. Powalla, Effects of heavy alkali elements in $Cu(In,Ga)Se_2$ solar cells with efficiencies up to 22.6%, Phys. Status Solidi RRL **10**, 583 (2016).

[6] M. Malitckaya, H.-P. Komsa, V. Havu, and M. J. Puska, Effect of alkali metal atom doping on the $CuInSe_2$-based solar cell absorber, J. Phys. Chem. C **121**, 15516 (2017).

[7] M. Malitckaya, T. Kunze, H.-P. Komsa, V. Havu, E. Handick, R. G. Wilks, M. Bär, and M. J. Puska, Alkali postdeposition treatment-induced changes of the chemical and electronic structure of $Cu(In,Ga)Se_2$ thin-film solar cell absorbers: A first-principle perspective, ACS Appl. Mater. Interfaces **11**, 3024 (2019).

[8] D. Hariskos, M. Ruckh, U. Rühle, T. Walter, H. W. Schock, J. Hedström, and L. Stolt, A novel cadmium free buffer layer for $Cu(In,Ga)Se_2$ based solar cells, Sol. Energy Mater. Sol. Cells **41-42**, 345 (1996).

[9] S. Siebentritt, Alternative buffers for chalcopyrite solar cells, Solar Energy **77**, 767 (2004), Thin Film PV.

[10] N. Naghavi, D. Abou-Ras, N. Allsop, N. Barreau, S. Bücheler, A. Ennaoui, C.-H. Fischer, C. Guillen, D. Hariskos, J. Herrero, R. Klenk, K. Kushiya, D. Lincot, R. Menner, T. Nakada, C. Platzer-Björkman, S. Spiering, A. N. Tiwari, and T. Törndahl, Buffer layers and transparent conducting oxides for chalcopyrite $Cu(In, Ga)(S, Se)_2$ based thin film photovoltaics: Present status and current developments, Prog. Photovolt: Res. Appl. **18**, 411 (2010).

[11] T. Minemoto, T. Matsui, H. Takakura, Y. Hamakawa, T. Negami, Y. Hashimoto, T. Uenoyama, and M. Kitagawa, Theoretical analysis of the effect of conduction band offset of window/CIS layers on performance of CIS solar cells using device simulation, Sol. Energy Mater. Sol. Cells **67**, 83 (2001), PVSEC 11-PART III.

[12] M. Morkel, L. Weinhardt, B. Lohmüller, C. Heske, E. Umbach, W. Riedl, S. Zweigart, and F. Karg, Flat conduction-band alignment at the $CdS/CuInSe_2$ thin-film solar-cell heterojunction, Appl. Phys. Lett. **79**, 4482 (2001).

[13] L. Weinhardt, O. Fuchs, D. Groß, G. Storch, E. Umbach, N. G. Dhere, A. A. Kadam, S. S. Kulkarni, and C. Heske, Band alignment at the $CdS/Cu(In, Ga)S_2$ interface in thin-film solar cells, Appl. Phys. Lett. **86**, 062109 (2005).

[14] Y. Hinuma, F. Oba, Y. Kumagai, and I. Tanaka, Band offsets of $CuInSe_2$/CdS and $CuInSe_2$/ZnS (110) interfaces: A hybrid density functional theory study, Phys. Rev. B **88**, 035305 (2013).

[15] T. Schulmeyer, A. Klein, R. Kniese, and M. Powalla, Band offset at the $CuGaSe_2/In_2S_3$ heterointerface, Appl. Phys. Lett. **85**, 961 (2004).

[16] P. Pistor, N. Allsop, W. Braun, R. Caballero, C. Camus, Ch.-H. Fischer, M. Gorgoi, A. Grimm, B. Johnson, T. Kropp, I. Lauermann, S. Lehmann, H. Mönig, S. Schorr, A. Weber, and R. Klenk, Cu in $In_2S_3$: Interdiffusion phenomena analysed by high kinetic energy x-ray photoelectron spectroscopy, Phys. Status Solidi A **206**, 1059 (2009).

[17] M. Bär, N. Allsop, I. Lauermann, and Ch.-H. Fischer, Deposition of $In_2S_3$ on $Cu(In, Ga)(S, Se)_2$ thin film solar cell absorbers by spray ion layer gas reaction: Evidence of strong interfacial diffusion, Appl. Phys. Lett. **90**, 132118 (2007).

[18] M. Bär, N. Barreau, F. Couzinie-Devy, S. Pookpanratana, J. Klaer, M. Blum, Y. Zhang, W. Yang, J. D. Denlinger, H.-W. Schock, L. Weinhardt, J. Kessler, and C. Heske, Nondestructive depth-resolved spectroscopic investigation of the heavily intermixed $In_2S_3/Cu(In,Ga)Se_2$ interface, Appl. Phys. Lett. **96**, 184101 (2010).

[19] O. Cojocaru-Miredin, Y. Fu, A. Kostka, R. Saez-Araoz, A. Beyer, N. Knaub, K. Volz, C.-H. Fischer, and D. Raabe, Interface engineering and characterization at the atomic-scale of pure and mixed ion layer gas reaction buffer layers in chalcopyrite thin-film solar cells, Prog. Photovolt: Res. Appl. **23**, 705 (2015).

[20] D. Hauschild, F. Meyer, A. Benkert, D. Kreikemeyer-Lorenzo, T. Dalibor, J. Palm, M. Blum, W. Yang, R. G. Wilks, M. Bär, F. Reinert, C. Heske, and L. Weinhardt, Improving performance by Na doping of a buffer layer–chemical and electronic structure of the $In_xS_y$: Na/$CuIn(S, Se)_2$ thin-film solar cell interface, Prog. Photovolt: Res. Appl. **26**, 359 (2018).

[21] E. Ghorbani and K. Albe, Influence of Cu and Na incorporation on the thermodynamic stability and electronic properties of $\beta$-$In_2S_3$, J. Mater. Chem. C **6**, 7226 (2018).

[22] M. Bär, N. Barreau, F. Couzinie-Devy, L. Weinhardt, R. G. Wilks, J. Kessler, and C. Heske, Impact of annealing-induced intermixing on the electronic level alignment at the $In_2S_3/Cu(In,Ga)Se_2$ thin-film solar cell interface, ACS Appl. Mater. Interfaces **8**, 2120 (2016).

[23] W. Paszkowicz, R. Lewandowska, and R. Bacewicz, Rietveld refinement for $CuInSe_2$ and $CuIn_3Se_5$, J. Alloys Compd. **362**, 241 (2004), proceedings of the Sixth International School and Symposium on Synchrotron Radiation in Natural Science (ISSRNS).

[24] R. Scheer and H. W. Schock, *Chalcogenide Photovoltaics: Physics, Technologies, and Thin Film Devices* (Wiley-VCH Verlag, Weinheim, 2011).

[25] C. Rincon, S. M. Wasim, G. Marin, R. Marquez, L. Nieves, G. S. Perez, and E. Medina, Temperature dependence of the optical energy gap and Urbach's energy of $CuIn_5Se_8$, J. Appl. Phys. **90**, 4423 (2001).

[26] L. Durán, C. Guerrero, E. Hernández, J. M. Delgado, J. Contreras, S. M. Wasim, and C. A. Durante Rincón, Structural, optical and electrical properties of $CuIn_5Se_8$ and $CuGa_5Se_8$, J. Phys. Chem. Solids **64**, 1907 (2003), 13th International Conference on Ternary and Multinary Compounds.

[27] N. Barreau, C. Deudon, A. Lafond, S. Gall, and J. Kessler, A study of bulk $Na_xCu_{1-x}In_5S_8$ and its impact on the Cu(In,Ga)$Se_2$/$In_2S_3$ interface of solar cells, Sol. Energy Mater. Sol. Cells **90**, 1840 (2006).

[28] P. Pistor, J. M. Merino Alvarez, M. Leon, M. Di Michiel, S. Schorr, R. Klenk, and S. Lehmann, Structure reinvestigation of $\alpha$-, $\beta$- and $\gamma$-$In_2S_3$, Acta Crystallogr., Sect. B **72**, 410 (2016).

[29] W. Rehwald and G. Harbeke, On the conduction mechanism in single crystal $\beta$-indium sulfide $In_2S_3$, J. Phys. Chem. Solids **26**, 1309 (1965).

[30] J. Heyd, G. E. Scuseria, and M. Ernzerhof, Hybrid functionals based on a screened coulomb potential, J. Chem. Phys. **118**, 8207 (2003).

[31] G. Kresse and J. Furthmuller, Efficient iterative schemes for ab initio total-energy calculations using a plane-wave basis set, Phys. Rev. B **54**, 11169 (1996).

[32] G. Kresse and J. Furthmueller, Efficiency of ab-initio total energy calculations for metals and semiconductors using a plane-wave basis set, Comput. Mater. Sci. **6**, 15 (1996).

[33] J. Pohl and K. Albe, Intrinsic point defects in $CuInSe_2$ and $CuGaSe_2$ as seen via screened-exchange hybrid density functional theory, Phys. Rev. B **87**, 245203 (2013).

[34] J. Pohl and K. Albe, Thermodynamics and kinetics of the copper vacancy in $CuInSe_2$, $CuGaSe_2$, $CuInS_2$, and $CuGaS_2$ from screened-exchange hybrid density functional theory, J. Appl. Phys. **108**, 023509 (2010).

[35] E. Ghorbani, J. Kiss, H. Mirhosseini, G. Roma, M. Schmidt, J. Windeln, T. D. Kühne, and C. Felser, Hybrid-functional calculations on the incorporation of Na and K impurities into the $CuInSe_2$ and $CuIn_5Se_8$ solar-cell materials, J. Phys. Chem. C **119**, 25197 (2015).

[36] E. Ghorbani and K. Albe, Intrinsic point defects in $\beta$-$In_2S_3$ studied by means of hybrid density-functional theory, J. Appl. Phys. **123**, 103103 (2018).

[37] Y. Hinuma, F. Oba, Y. Kumagai, and I. Tanaka, Ionization potentials of (112) and $(11\bar{2})$ facet surfaces of $CuInSe_2$ and $CuGaSe_2$, Phys. Rev. B **86**, 245433 (2012).

[38] N. Barreau, Indium sulfide and relatives in the world of photovoltaics, Solar Energy **83**, 363 (2009).

[39] J. E. Jaffe and A. Zunger, Electronic structure of the ternary chalcopyrite semiconductors $CuAlS_2$, $CuGaS_2$, $CuInS_2$, $CuAlSe_2$, $CuGaSe_2$, and $CuInSe_2$, Phys. Rev. B **28**, 5822 (1983).

[40] J. Kiss, T. Gruhn, G. Roma, and C. Felser, Theoretical study on the structure and energetics of Cd insertion and Cu depletion of $CuIn_5Se_8$, J. Phys. Chem. C **117**, 10892 (2013).

[41] S. B. Zhang, S.-H. Wei, A. Zunger, and H. Katayama-Yoshida, Defect physics of the $CuInSe_2$ chalcopyrite semiconductor, Phys. Rev. B **57**, 9642 (1998).

[42] S.-H. Wei and A. Zunger, Band offsets and optical bowings of chalcopyrites and Zn-based II-VI alloys, J. Appl. Phys. **78**, 3846 (1995).

[43] M. Turcu, I. M. Kötschau, and U. Rau, Composition dependence of defect energies and band alignments in the $Cu(In_{1-x}Ga_x)(Se_{1-y}S_y)_2$ alloy system, J. Appl. Phys. **91**, 1391 (2002).

[44] S.-H. Wei and A. Zunger, Calculated natural band offsets of all II-VI and III-V semiconductors: Chemical trends and the role of cation *d* orbitals, Appl. Phys. Lett. **72**, 2011 (1998).

[45] D. Schmid, M. Ruckh, F. Grunwald, and H. W. Schock, Chalcopyrite/defect chalcopyrite heterojunctions on the basis of $CuInSe_2$, J. Appl. Phys. **73**, 2902 (1993).

[46] D. Liao and A. Rockett, Cu depletion at the $CuInSe_2$ surface, Appl. Phys. Lett. **82**, 2829 (2003).

[47] M. Bär, S. Nishiwaki, L. Weinhardt, S. Pookpanratana, O. Fuchs, M. Blum, W. Yang, J. D. Denlinger, W. N. Shafarman, and C. Heske, Depth-resolved band gap in Cu(In, Ga)(S, Se)$_2$ thin films, Appl. Phys. Lett. **93**, 244103 (2008).

[48] A. Hofmann and C. Pettenkofer, The $CuInSe_2$-$CuIn_3Se_5$ defect compound interface: Electronic structure and band alignment, Appl. Phys. Lett. **101**, 062108 (2012).

[49] M. Mezher, L. M. Mansfield, K. Horsley, M. Blum, R. Wieting, L. Weinhardt, K. Ramanathan, and C. Heske, Kf post-deposition treatment of industrial Cu(In, Ga)(S, Se)$_2$ thin-film surfaces: Modifying the chemical and electronic structure, Appl. Phys. Lett. **111**, 071601 (2017).

[50] J. R. Tuttle, D. S. Albin, and R. Noufi, Thoughts on the microstructure of polycrystalline thin film $CuInSe_2$ and its impact on material and device performance, Solar Cells **30**, 21 (1991).

[51] M. Städele, J. A. Majewski, and P. Vogl, Stability and band offsets of polar GaN/SiC(001) and AlN/SiC(001) interfaces, Phys. Rev. B **56**, 6911 (1997).

[52] C. G. Van de Walle and J. Neugebauer, Universal alignment of hydrogen levels in semiconductors, insulators and solutions, Nature (London) **423**, 626 (2003).

[53] A. Schleife, F. Fuchs, C. Rödl, J. Furthmüller, and F. Bechstedt, Branch-point energies and band discontinuities of III-nitrides and III-/II-oxides from quasiparticle band-structure calculations, Appl. Phys. Lett. **94**, 012104 (2009).

[54] H. Peelaers, D. Steiauf, J. B. Varley, A. Janotti, and C. G. Van de Walle, $(In_xGa_{1-x})_2O_3$ alloys for transparent electronics, Phys. Rev. B **92**, 085206 (2015).

[55] N. Naghavi, R. Henriquez, V. Laptev, and D. Lincot, Growth studies and characterisation of $In_2S_3$ thin films deposited by atomic layer deposition (ALD), Appl. Surf. Sci. **222**, 65 (2004).

[56] A. Klein, Energy band alignment at interfaces of semiconducting oxides: A review of experimental determination using photoelectron spectroscopy and comparison with theoretical predictions by the electron affinity rule, charge neutrality levels, and the common anion rule, Thin Solid Films **520**, 3721 (2012), 7th International Symposium on Transparent Oxide Thin Films for Electronics and Optics (TOEO-7).

[57] J. B. Varley and V. Lordi, Electrical properties of point defects in CdS and ZnS, Appl. Phys. Lett. **103**, 102103 (2013).